Estimating the value of demand-side management in low-cost, solar micro-grids

Energy 163 (2018) 74–87

Contents lists available at ScienceDirect

Energy

journal homepage: www.elsevier.com/locate/energy

Estimating the value of demand-side management in low-cost, solar micro-grids

Varun Mehra*, Reja Amatya, Rajeev J. Ram

Tata Center for Technology and Design, Massachusetts Institute of Technology, United States

ARTICLE INFO

Article history:
Received 3 April 2017
Received in revised form
14 July 2018
Accepted 30 July 2018
Available online 6 August 2018

Keywords:
Micro-grids
Electricity access
Demand-side management
Reliability
Asset selection
Off-grid
Techno-economic model
Cost

ABSTRACT

Demand-side management has the potential to reduce the cost of solar based community micro-grids and solar home systems for electricity access. This paper presents a methodology for optimal least-cost sizing of generation assets while meeting explicit reliability constraints in micro-grids that are capable of active demand management. The battery management model considers kinetic constraints on battery operation and represents dispatch in the field to regulate the depth of discharge. The model allows consideration of the trade-off between depth of discharge, cycle life, and calendar lifetime in lead-acid batteries. Separate reliability targets for disaggregated, residential load profiles at hourly timesteps are considered to evaluate the performance and cost reduction potential of demand-side management capabilities — with economic results and sensitivity analyses around key input assumptions subsequently presented. We find that demand-side management can reduce the number and cost of requisite solar panels and batteries with the integration of real-time management and controls – a key result for justifying next generation micro-grids for electricity access.

1. Introduction

Over one billion people mostly in developing countries live without electricity access, and many who have grid-connections are subject to low levels of reliability and poor quality of service. In India alone, it is estimated that 300 million people lack basic electricity access [1]. Access to electricity has been inextricably linked to human development, as many studies have documented this over a wide range of development indicators such as life expectancy at birth, education, literacy etc. [1]. With the immediate challenges of minimizing greenhouse gas emissions from the power sector, and at the same time serving increasing population, affordable and distributed renewable energy sources are required to achieve the United Nations' Sustainable Development Goal for universal energy access. Solar-based community micro-grids and individual home systems have been recognized as key enablers of electricity provision to many living without access to-date.

Despite significant cost reductions in solar panels in recent years, both individual solar home systems and micro-grids can still be cost-prohibitive for people in developing countries. Most solar-based off-grid systems in such rural communities either have batteries that are over-sized to ensure reliability and autonomous operation for 3–5 days or back-up diesel generators — both of which can add to the overall system costs. In addition, utilization of smaller panels (which have higher per unit costs) and requirements for individualized maintenance also increases the cost for solar home systems [1]. At a much larger scale, micro-grids in rural villages typically require community buy-in, which forces a flat tariff on service providers and drives up the cost of customer acquisition [2]. In regards to micro-grid system operation — load curtailment, revenue collection, and theft monitoring are major issues that drive up the cost with conventional micro-grid approaches and installations [3].

Recent adoption, deployment, and financial sustainability of off-grid electricity services have been boosted by technologies equipped as a “utility-in-a-box” solution, which seem to help alleviate issues seen today with conventional off-grid systems [3]. The recent advent of intelligent devices and low-cost computation have enabled such “utility-in-a-box” solutions in various ways by implementing smart demand-side management [4] and network controls [5]. A key motivating factor for deployment of such technologies is the ability to build a network from a bottom-up approach, while also taking advantage of economies of scale seen

* Corresponding author.
E-mail address: varunm@alum.mit.edu (V. Mehra).

https://doi.org/10.1016/j.energy.2018.07.204
0360-5442/

Nomenclature

B	Battery capacity (Amp-hours)
C	Cash outflows ($)
c	Generation asset cost ($)
CD	Cumulative electricity demand of critical load profile (kWh-year)
CL	Battery cycle life (number of cycles)
CP	Critical load profile (kW)
CR	Reliability of critical load profile (%)
d	Yearly discount rate (%)
d'	Monthly discount rate (%)
ESC	Cumulative electricity served of critical load profile (kWh-year)
EST	Cumulative electricity served of total load profile (kWh-year)
h	Number of households
i	Hour of year index (1 … 8760)
j	Household number index (1 … h)
k	Battery capacity index (1 … n)
l	Solar panel index (1 … m)
$LCOE$	Levelized cost of electricity ($/kWh)
m	Number of solar panels
$MDOD$	Maximum depth of battery discharge (%)
n	Number of batteries
NPV	Net present value ($)
PV	Solar panel capacity (Watts)
q_1	Available battery capacity (kW)
q_2	Bound battery capacity (kW)
q_{total}	Total battery capacity (kW)
TD	Cumulative electricity demand of total load profile (kWh-year)
TP	Total load profile (kW)
TR	Reliability of total load profile (%)
V	Battery voltage (Volts)
Y	System lifetime (years)
y	Year index (1 … Y)

from connecting households to a central solar panel and battery — potentially overcoming challenges of village-scale customer acquisition and other issues common in conventional micro-grids [3]. This approach can also enable new, and innovative business models for electrification [2]; for example with modular systems and autonomous operation, individuals in off-grid areas can monetize investments in their own electricity infrastructure.

Power management strategies in resource-constrained, isolated solar micro-grids can manage both the real-time availability of electricity supply and expectation of electricity demand; examples of advanced algorithms for real-time operation of micro-grids using recurring load forecasts can be found in Refs. [6] and [7], for managing varying characteristics of generating sources in Ref. [8], and for electricity scheduling to guarantee reliability in Ref. [9]. The key interest of this work is to illustrate that micro-grids with demand-side management can alleviate some cost challenges with conventional electrification approaches. The network architecture in Ref. [10] considers smaller units of 5–10 households as nano-grids that can build a larger network, and such systems can take advantage of economies of scale by drawing from the same solar panel and battery — thus avoiding traditional hurdles in acquiring customers at once and placement of solar arrays and battery banks in a conventional micro-grid setup.

The main focus of this paper is to analyze one such concept of interconnected network – a nano-grid in this case: on the order of 5–10 households, based on the capabilities assumed and described in a "utility-in-a-box"-type solution designed for electricity access in Ref. [10]. This paper presents a framework containing both technical and economical parameters to illustrate the value of power management devices with demand-side management capabilities in such off-grid systems. The model allows for effective selection of generation assets based on predefined criteria, such as target reliability and/or system costs. Basic operational characteristics of a solar-based off-grid system is incorporated in the model by taking into account operation of all major components including solar generation, battery operation, network efficiency losses, and dispatch decisions that correspond to demand estimates that reflect real off-grid systems. The latter part of this paper explains how the technical simulations for a micro-grid with demand-side management translates to economic viability and financial analysis based on the optimization of generation asset sizes.

Previous techno-economic modeling approaches for micro-grids tend to be narrowly focused on specific geographies (for example in rural Nigeria in Ref. [11] and for a Greek island in Ref. [12]) and/or with overly-specific choices in generation sources (for example with a "biogas–diesel–battery hybrid energy system" in Ref. [13], with a "photovoltaic, wind, diesel and hybrid electrification system" in Ref. [14], and with a "battery/hydrogen" hybrid power system in Ref. [15]). Such approaches also describe optimal generation asset sizing techniques using combinations of generation sources not readily available or relevant in electricity access contexts, and are designed to provide very high levels of system reliability by keeping demand fixed.

Other approaches have analyzed the effects of a subset of aspects related to micro-grid operations on costs, such as with modeling various business model operational parameters in Ref. [16] or discount/interest rates in Ref. [17] — but have not incorporated them holistically from technical performance to economic/financial analysis. This also extends to the inclusion of key operational parameters from a micro-grid company's perspective, such as equipment operation, replacement costs, investment parameters, etc. The work presented here uses the state of Jharkhand, India to ground analyses with realistic parameters, but the structure of this comprehensive techno-economic modeling approach can be extrapolated to other contexts given changes in input assumptions such as solar irradiance, demand profiles, and generation asset availability.

The remainder of the paper is structured as follows. Section 2 provides an overview and process flow description of the model constructed – with Section 3 focusing on the reliability metric used, which is the key decision variable in the model in the selection of optimal, least-cost generation assets. Section 4 describes the method for constructing disaggregated critical and non-critical demand profiles at the household level, while Section 5 describes the technical details of the micro-grid network architecture (e.g. DC/DC converter efficiencies, wiring losses, solar module power output, and lead-acid battery operation), along with the dispatch heuristic used. Sections 6 and 7 introduce the available state-space of solar/battery combinations and the optimal selection of generation asset selection that meet reliability constraints based on simulations. These results are extrapolated to the cost and financial analysis of the modeled micro-grid in Section 8, with Section 9 subjecting key input assumptions of the model to sensitivity analysis for deeper insight. Section 10 compares the generation

asset size method to conventional systems and evaluates the capital cost benefit for micro-grids with demand-side management capabilities based on the use-case presented – with concluding remarks shared in Section 11.

2. Model approach & objective

The advent of low-cost computation, power electronics, and sensors – integrated into power management devices – can enable the next generation of micro-grids for rural electrification. These capabilities can allow for a variety of power management strategies and can be integrated in a distributed, 'prosumer' network architecture, as described in Ref. [10] for example. While typical micro-grids provide fixed hours of evening electricity services, effective real-time demand-side management based on load disaggregation can differentiate critical and non-critical loads, and can regulate the amount of power consumed during operation to maintain network reliability.

The motivation for conducting this technical analysis is to identify the optimal, least-cost, combination of solar and battery assets that meet reliability constraints given the demand management capabilities of a system. In order to come up with values for reliability and assess the performance of various solar and battery combinations, key components of the network such as wiring losses, DC/DC converter efficiency, solar module power production, and battery operating constraints have been modeled appropriately. As a reference, the process flow of the model constructed, from initialization of key parameters/inputs to optimizing solar and lead-acid battery selections to an economic/financial analysis is illustrated in Fig. 1, with details on each input and computational step further discussed in Sections 4–7.

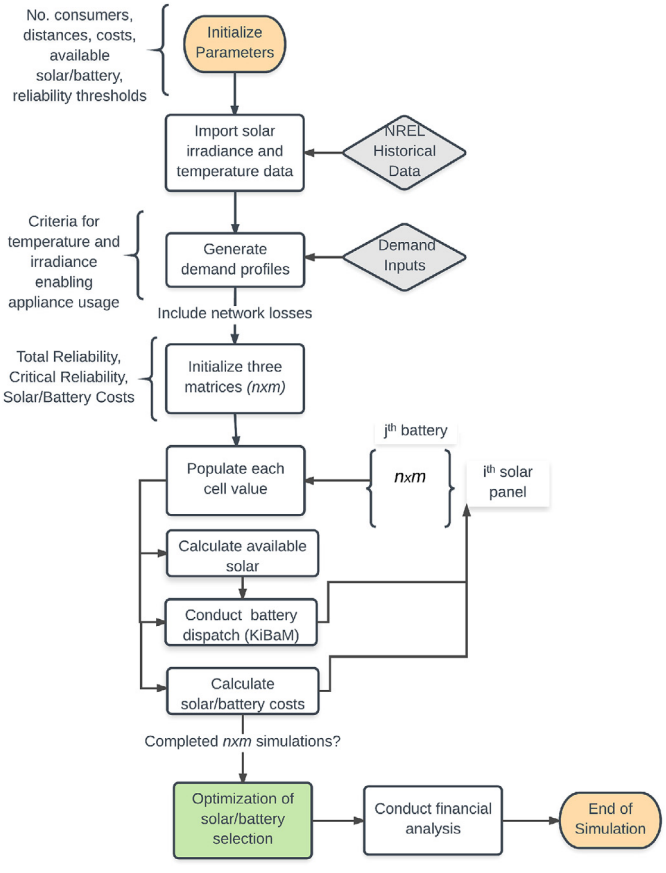

Fig. 1. Process flow diagram for constructed model.

Operational simulation of power systems is an active field of research, and numerous software programs and commercial packages have been introduced in recent years that translate detailed engineering models to system design and overall economics. These software platforms, such as 'Hybrid Optimization of Multiple Energy Resources' (HOMER) and 'Distributed Energy Resources — Consumer Adoption Model' (DER-CAM), can be used to assess the sizing and model the performance of distributed energy technologies (such as fuel cells, diesel generators, photovoltaics, batteries, etc.) over a period of time in a specified geographic area.

This modeling approach relies on the formulation of a well-known Kinetic Battery Model (KiBaM) [18]. The model has been adapted to include dynamic battery management constraints that is tied to rates of charge, discharge, and depth of discharge to more realistically represent a real-time operation. In contrast with previous use-cases of the KiBaM model [19], the explicit inclusion of depth of discharge as a model input allows the consideration of trade-offs between depth of discharge, cycle life, and calendar lifetime in a lead-acid battery.

The approach taken in this work also differs both in the methodology for constructing demand profiles and the considerations of meeting reliability thresholds by conducting demand side management. Previous work considers demand profile construction based on either data directly gathered from installations (for example via data collected from a micro-grid with a freezer load in Mali [20] and off-grid systems in Malawi [21] or based on household meter data as in Ref. [22]), or synthesized load profiles (for example using a back-of-the-envelope technique to estimate daily consumption as in Ref. [16] or Monte Carlo simulations across appliances' load profiles in Ref. [23]); in contrast, this work explicitly disaggregates synthesized load profiles based on separating critical and non-critical loads. This is coupled with the explicit consideration of separate target reliabilities for these disaggregated load profiles at hourly timesteps – a capability required to evaluate the performance and potential of on-site demand-side management. A version of the MATLAB code developed can be found in Ref. [24].

3. Definition of reliability metric

In the construction of most power system models, service reliability is a critical decision variable and metric. Considering that the reliability metric is the key determinant in the solar and battery asset sizes in this model, it is worth discussing and defining this metric explicitly. In centralized power systems, three common metrics are used – in SAIFI (system average interruption frequency index, in units of number of occurrences per customer per year), SAIDI (system average interruption duration index, in units of number of hours per customer per year), and ASAI (average service availability index, in percent of energy unavailable in reference to expected demand) are used [25]. Assigning values to reliability is not straight-forward, but can be inferred based on costs of event outage with an example using logarithmic regressions as in Ref. [26].

There have been a handful of papers focused on analyzing reliability in the context of distributed, off-grid systems. In Ref. [22], different combinations of solar/storage systems for an individual household are modeled using the HOMER micro-grid simulation software – with results showing higher costs for serving expected load (both when inputting deferrable and non-deferrable load profiles) for 99.99% versus 80%. In Ref. [27], reliability indicators are assessed for hybrid systems taking into account variability in wind and solar power generation – such as the loss of load probability (binary encoding if the entire load was served in a time period, integrated over all the time periods), which is similar to the energy supply probability metric used in Ref. [20].

The reliability metric used in the model presented here is the same as the ASAI metric; the way the reliability value is calculated is based on the ratio of the energy not served to the expected demand profile integrated over the entire year. This choice of a reliability metric yields the average reliability over the entire year, in percent. To provide clarity and insight, subsequently presented simulation results over an entire year will show the discrepancy between the average yearly reliability versus hourly reliability.

4. Demand load profile construction methodology

As explained in Ref. [28], understanding the demand profiles as a function of appliances and other variables, such as time of day and temperature, is of critical importance. In any power system, the choice of generation assets and assurance of resource adequacy is a function of the expected demand – whether aggregated at a feeder level, household-by-household, or appliance-by-appliance.

The model described here relies on the methods included in the Reference Electrification Model (REM) [29], which generates a randomized demand profile at each household given the number of consumers in the network based on appliance-level input assumptions. The REM takes inputs in from survey results on expected electricity consumption needs, and creates typical household energy consumption vectors of desired length in hours. The model randomly permutes start/end times of appliance activities drawing from a uniform distribution within predefined time ranges and also introduces day-to-day variability of amount of electricity usage. REM also allows for exogenous variables, such ambient temperature and sunlight levels, to induce fan and light usage, respectively [30]. The input variables are based on historical average irradiance and temperature data over a year timeframe – which can be obtained for a particular longitude and latitude from the National Renewable Energy Laboratory's (NREL) PVWatts database and calculator [31]. For the purposes of the use-case of this model presented herein, the geographical location and coordinate choice is the peri-urban area in the state of Jharkhand, India. This region has a favorable solar resource – on the order of ~ 5.0–5.5 kWh/m^2 per day [31].

The description of the loads (e.g. LED lights, fans, and mobile charger) per household used in this model are shown in Table 1 – along with assumptions on hourly usage and exogenous variables that would induce the appliance's usage (e.g. ambient temperature, amount of sunlight). The choice of loads is reasonably consistent with loads available from solar home systems from companies such as Tata Power Solar and SELCO in India. As part of this effort, a binary encoding of critical (1) and non-critical (0) loads are additional inputs into the demand profile construction, representing the ability to disaggregate individual loads. Each household's demand profile is separated into two 8760 element vectors (hours in a year), for critical and total load profiles, and is then integrated across the number of consumers in the network. Note that the generic nature of this model can allow for different load priorities and a larger number/higher diversity of loads to model additional use-cases.

Fig. 2 shows the effect that the 'enabled when' criterion has on the generation of load profiles over simulated hours. The top plot shows the influence of the ambient temperature on the fan usage – when above 31 °C, while the lower plot shows how low solar irradiance triggers the light usage – when below 5 W/m^2. Again, each of the demand profiles are generated one user at a time for each hour of the year ($i = 1 \ldots 8760$), and then a cumulative load profile for the whole network is generated by recursively adding each household's (user's) load profile together ($j = 1 \ldots h$). Example of an individual household's demand profile ($TP_{i,j}$) is shown in Fig. 3, with the cumulative total load profile (TP_i) integrated across the network for an entire year; note that the equations that follow also hold for the critical demand profile (CP). Its important to note that due to the introduction of randomness, the household-level demand profiles are not deterministic and are also not perfectly correlated with each other.

5. Description of technical aspects of model

5.1. Network architecture & power management devices

The direct current (DC) network architecture was chosen to be modeled in this effort due to low demand requirement on the ground, and for explicit reliance on integrating low-cost DC components for this application. Each modular unit of 5–10 households would consist of generation (solar panels), storage (lead-acid batteries), wiring, and power management devices at the network and household levels. Specifically, there are two types of power

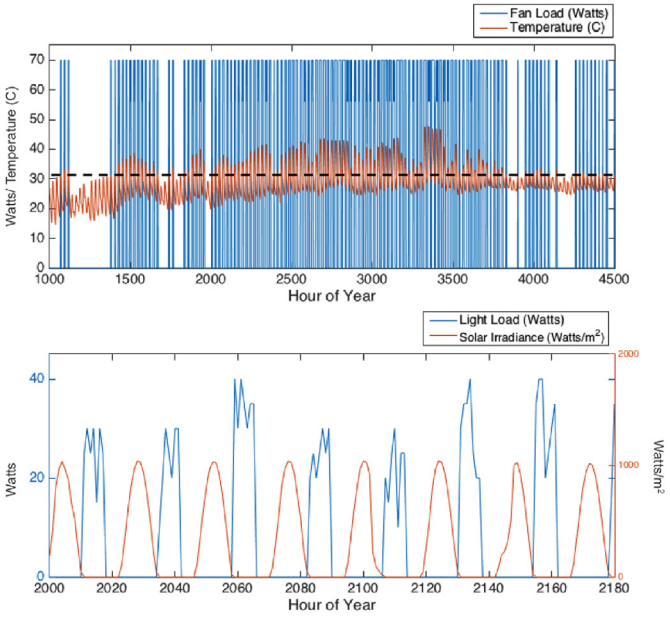

Fig. 2. Example of fan and lighting load conditioned on ambient temperature and sunlight.

Table 1
Demand load profile inputs: Residential load scenario.

Parameters	Appliance		
	Light (LED)	Fan	Cell Phone Charger
Number	2	1	1
Hours per Day	4	4	4
Watts	5	14	2.5
Critical (Y/N)	Y	N	N
Enabled	Irradiance ≤ 0.05 W/m^2	Temp ≥ 31°C	N/A

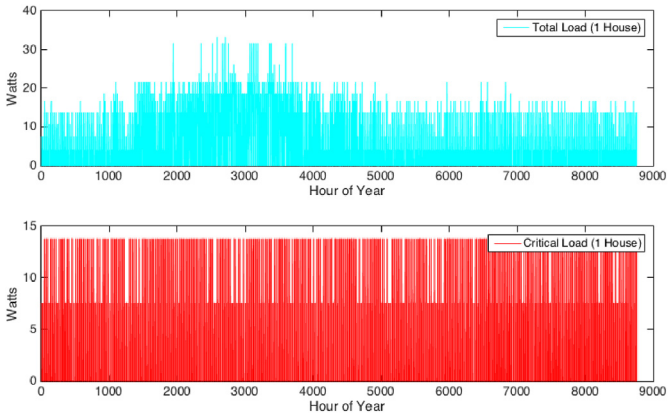

Fig. 3. Example of total and critical yearly load profile for one household.

management devices considered here. The generator device (also referred to as 'source') would consist of an MPPT (maximum power point tracking) charge controller, a boost converter to a 24 V DC network – with multiple outputs to connect either a bus or individual households. The generator device includes local memory and a micro-processor, and bi-directional communication can take place between the generator device and consumer devices [10]. At each household, the consumer device (also referred to as the 'load' device) consists of a single-input, multi-output buck converter with current-control capabilities, switches, and sensors at each outlet. The relevant aspects included in the model are network topology, DC/DC converters' efficiencies, and wiring losses.

The overall network topology is depicted in Fig. 4, showing the layout of the source and load units relative to the solar panel, battery, network, and the end-user appliances. The selection of the specific DC/DC converter circuit topology, individual components (e.g. capacitors, transistors, inductors, thermal management, etc.) and logic embedded within (e.g. duty cycle, switching frequency, mode of operation) is driven by cost, efficiency, voltage range, and power levels desired. In the context of such ad-hoc DC micro-grids

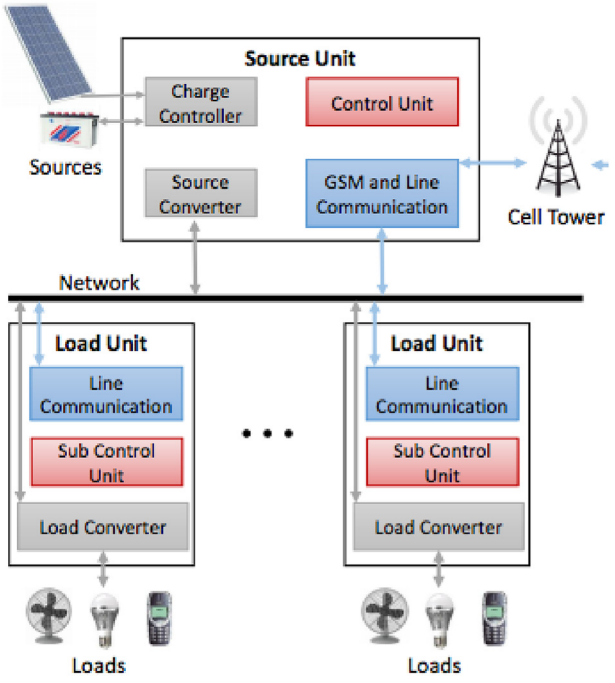

Fig. 4. Modelled architecture & proposed network layout [10].

with applications in electricity access, the subject of designing safe, reliable, and low-cost power electronics is conducted in Ref. [32], with analysis on transient stability of voltage and power due to load switching is discussed in Ref. [33].

5.2. Battery model and dispatch constraints

In India, lead-acid still remains the most widely available, well-understood, and popular battery chemistry across many applications (e.g. uninterruptable power supplies (UPS), urban power back-up, etc.) – hence its choice for modeling purposes herein. A detailed discussion of battery modeling is outside the scope of this paper, but is the subject of review and detailed analysis in Ref. [28]. The work presented here focuses on the adaptation of the Kinetic Battery Model (KiBaM), originally conceived of in Ref. [18]. Specifically, the implementation consists of the key operating constraints to simulate battery management and dispatch in a micro-grid, given a net current profile of solar irradiance and demand. The KiBaM effectively represents the charge that is both available and inaccessible due underlying electrochemical phenomena (e.g. formation of concentration gradients that impact mass transport of ions to electrodes, where oxidation (discharge) or reduction (charge) reactions take place). Visually speaking, the KiBaM can be described in a two-tank model to show that there is only a certain amount of accessible battery capacity in the battery at each time step. This value is based on the accessible capacity in the previous time step and the input/output current desired at each time step, subject to charge/discharge constraints [18].

To use the KiBaM to simulate the real-time operation of a battery and a local controller's dispatch heuristic, equations need to be solved to obtain values for available capacity (defined as q_1) and bound capacity (defined as q_2) at each time step by feeding in the net current profile based on a nominal battery voltage, which is assumed to be 12 V for lead-acid batteries. The original KiBaM also includes input and output current constraints, calculated separately for charging and discharging, that set maximum limits on how much current the battery can input or output at each time step [18]. In this case, the current profile is a vector of 8760 elements, which is equal to the net power profile (total load minus available solar), divided by the nominal battery voltage. Note that the net incident solar power is module size and irradiance dependent, and the load profile construction is dependent on a number of factors described previously and in Ref. [28].

For illustrative purposes, an example of the solar and load profiles and the KiBaM variable outputs (q_1, q_2, and q_{total}) are shown in Fig. 5; these outputs are based on the net current profile from a 120 W solar panel, a 75 Ah battery, and a residential load profile across 5 households; note that the assumptions in determining the solar power output and load profile construction models that populate these vectors are consistent with the methods described herein. During roughly the hours 2000–4000 (essentially March–June), the load profile increases due to the increase in fan usage – induced by the ambient temperature – which affects the available charge in the battery. There is also a period after hour 4000 where the available solar decreases due to the monsoon season, but the presence of evening lighting loads is not a large enough load, in this example, to keep the battery capacity low during this period of low irradiance. This is further supported by the outputs in Fig. 6, which indicates the calculated values of each discharging (top plot) and charging (bottom plot) constraint during each time step over a simulated year.

In this model, the dispatch heuristic is based on the instantaneous availability of solar generation, battery capacity, and demand – at each time step. Table 2 shows the number of hours each constraint is reached for both charging and discharging. For

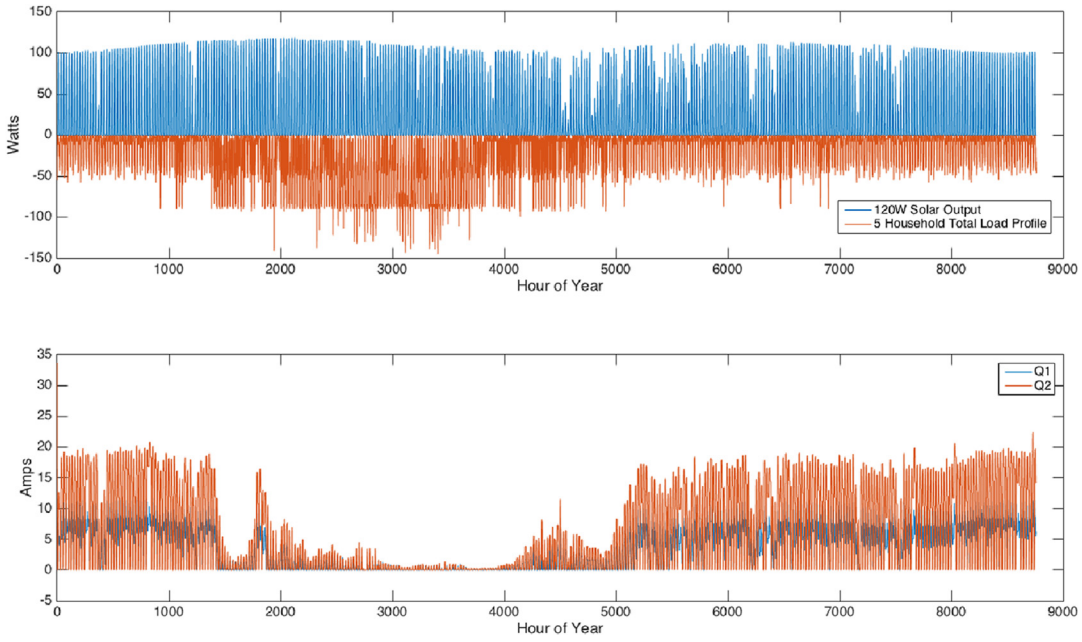

Fig. 5. Example of net load profile and KiBaM variable outputs.

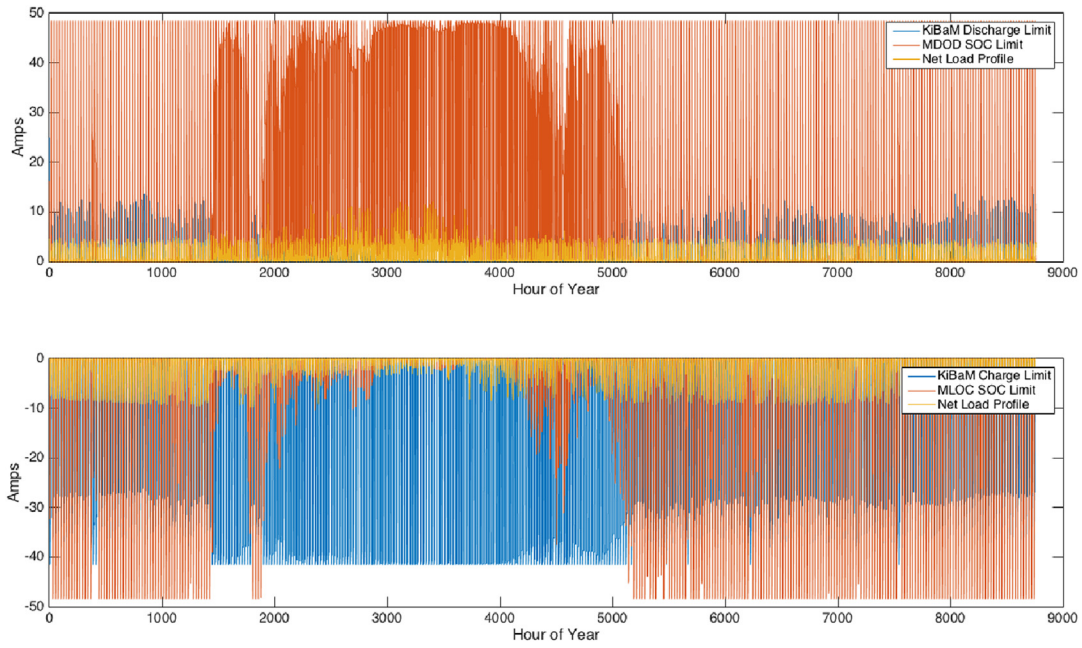

Fig. 6. Example of charging and discharging KiBaM constraints.

illustrative purposes, this particular instantiation of the model is with a 120 W panel and a 75 Ah battery, serving 5 residential households; the 'Net Load' is either the net solar during charge, or the net load during discharge.

Table 2
Example of number of hours KiBaM charge and discharge constraints reached.

Constraint	Charge	Discharge
Net Load	1159 (77%)	567 (12.6%)
KiBaM Constraint	0 (0%)	2993 (66.6%)
SOC Constraint	2428 (67.7%)	935 (20.8%)
Total Hours	3587 (40.9%)	4495 (51.3%)

In this simulation, the KiBaM charge constraint is never reached during the hours that the battery is charging. This is due to the fact that the rate of solar energy charging the battery is never high enough to force the KiBaM charge constraint to be reached – but there are numerous hours where the additional SOC constraint is reached (2,428), indicating the presence of spillage (i.e. excess and unusable solar generation). However, during discharge, the KiBaM discharge constraint is the most frequent constraint reached, indicating that the battery was not able to serve the rate of discharge required by the load for 2993 h; furthermore, the net load was only served in its entirety 567 of the 4495 h the battery was discharging over the year. This is supported by the fact that for this

configuration, the average yearly reliability is low, calculated to be 56.3%.

5.3. Battery cycle life

For modeling purposes, counting battery cycles is a value dependent on the incident load and solar profile that is discharging and charging the battery. The ability to count cycles can allow for a model to better estimate when a battery has reached its end-of-life based on the rated cycle life, which impacts the replacement costs over the system's lifetime (the economic implications of which are further discussed). To implement such a method, the rainflow counting algorithm is used to track the number of cycles based on using the battery's historical SOC over one year [34].

Regardless of the rated cycle life of a battery, how it is operated in the field can have a significant effect on its lifetime. Some battery manufacturers provide data relating the cycle life to the depth of discharge; the depth of allowable discharge directly relates to the number of cycles that a lead-acid battery can realistically withstand over the lifetime of its usage. In 12 V lead-acid batteries, rule of thumb is to not discharge beyond 50%–60%; excessive discharge can increase sulphation of the electrodes, decreasing the available electrode area for reactions to take place and thus the effective capacity.

$$CL = 5,891e^{(-2.382\times MDOD)} \quad (1)$$

Examples of lead-acid batteries' cycle life (CL) as a function of its maximum depth of discharge ($MDOD$), based on a handful of data points gathered from lead-acid battery manufacturers in India, is seen in Fig. 7. The MDOD factor is a key input to the model, with the cycle life of a battery dictated by the choice of MDOD; the sensitivity to this input parameter is discussed in more detail subsequently, but the default value for the purposes of the use-case shared herein assumes an MDOD of 60%, corresponding to a rounded value of 1400 cycles per exponential fit described in Equation (1).

6. Description of economic aspects of model

6.1. Battery and solar combinations based on distributor availability & economies of scale

A key oversight of previous modeling approaches is that models based on strict optimization of battery and solar panel selection might identify a more optimal yet unavailable solution in terms of field implementation. In contrast, the modeling approach conducted for this analysis is focused on finding a least cost combination of solar panels and batteries to meet a certain level of demand reliability – dependent on locally available solar panels and batteries. Though there are many different sizes of solar panels, especially when looking across many manufacturers, not all of those increments (e.g. 10 W or 20 Ah) or combinations may be available in remote, rural areas. Thus, as an illustrative example, this modeling approach initializes the available state-space based on available Su-Kam solar panels (50 W–300 W) and Exide and Amara Raja battery capacities (60 Ah-200 Ah) from a local distributor in the city of Jamshedpur, India [28].

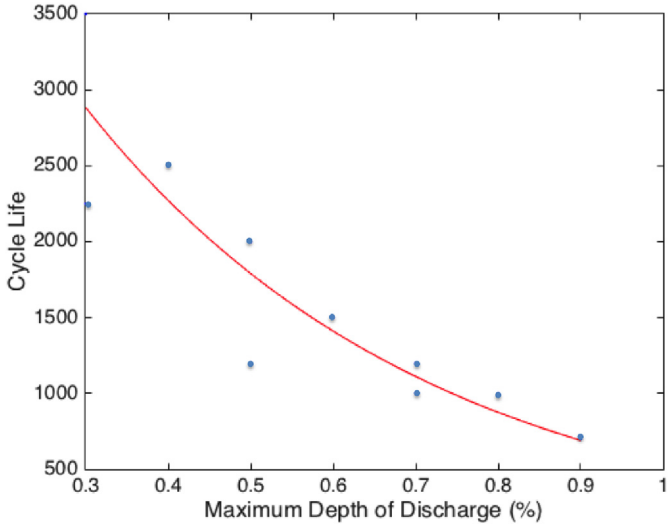

Fig. 7. Exponential fit of MDOD versus cycle life for available 60 Ah-200 Ah lead-acid batteries in Jharkhand, India.

Another rationale for building such nano-grids as opposed to individual solar home systems is to leverage economies of scale. As a result, both solar panels and batteries have a lower unit cost ($/W and $/kWh respectively) with increasing capacities. This model takes into account these aspects, with cost and availability data gathered directly from the local distributor. Again, including these aspects formulates the state space for available solar and battery combinations subject to reliability constraints, which is the key decision-making step in the model. As a reference, the two-term exponential fit equations describing the economies of scale for both solar panels ($\$/W$) and batteries ($\$/kWh$) are shown in Equations (2) and (3) below [28]:

$$\$/\text{kWh} = 288.8e^{-0.0868\times Ah} + 125.3e^{-0.0011\times Ah} \quad (2)$$

$$\$/\text{W} = 0.5689e^{-0.0487\times W} + 0.8098e^{-0.0001\times W} \quad (3)$$

6.2. Additional requisite micro-grid cost inputs

In order to conduct a complete cost analysis, the remaining bill-of-materials are tabulated in Table 3. The requisite power management network devices are split into 'generator' (source) and 'consumer' (load) devices. This nomenclature simply means that the generator device resides near the solar panel and the battery, and includes a charge controller along with local computation to manage the network. Consistent with the costs of the generation assets, the costs of other aspects required in building a micro-grid are based off of available prices from local appliance and electrical shops in the city of Jamshedpur, India. As Table 3 shows, additional cost inputs per household include wiring, power management devices, and appliances.

6.3. Costs of power management devices

For the generator device and consumer devices, the bill of materials is based on the analysis conducted in Ref. [32] for designing safe, reliable, and low-cost power electronic devices in the context of off-grid electricity access. For the generator device, key costs include components required for the power stage, micro-controller,

Table 3
Key cost inputs from Jamshedpur, India (June 2015).

Item	Cost (Rs.)	Cost ($)	Value
Electrical Wiring	Rs. 3.6/m	$0.06/m	40 m/household
Communication Wiring	Rs. 1.8/m	$0.03/m	40 m/household
LED Cost	Rs. 100/unit	$1.67/unit	4 units/household
Fan Cost	Rs. 600/unit	$10/unit	1 unit/household
Mobile Charger	Rs. 100/unit	$1.67/unit	1 unit/household
Generator Device	Rs. 2400/unit	$40/unit	1 unit/network
Consumer Device	Rs. 900/unit	$15/unit	1 unit/household
Pole	Rs. 200/unit	$3.33/unit	1 unit/household

sensors, printed circuit board, etc.; furthermore, the cost of the MPPT charge controller are also included – and the cost for the generator device at supplier scale (10,000 units) is estimated to be $40. For the consumer device, the key costs similarly include components required for the power stage, isolation/safety protection, sensors, etc. The cost for the consumer device at supplier scale (10,000 units) is estimated to be $15.

7. Optimal selection of generation asset selection subject to reliability constraints

The previous sections have discussed the technical representation of the key components included to model micro-grids of interest. Specifically, the paper thus far has detailed the representation of demand, network architecture, solar power generation, and lead-acid battery operational constraints. Before the cost and financial analysis, the key, final step of the model is to select the least cost combination of solar module and battery capacity in order to meet reliability thresholds.

The model computes the reliability over the entire year for both critical and total load profiles – populating each cell in a matrix for every available combination of battery (index k) and solar panel (index l). The discrete combinations of individual solar panels and battery capacities are based on a particular distributor's availability in Jamshedpur, India in order to constraint realistic solutions (and costs) for implementation in off-grid areas in Jharkhand as an example.

To recall, reliability is defined as the sum of the total load served divided by the total expected load over the entire year; in this modeling context, the load profile is assumed to be entirely known a priori but dispatch decisions are made every time step. Furthermore, the definition of reliability ($TR_{k,l}$ and $CR_{k,l}$, in %) per solar/battery combination is the total amount of electricity served (EST, ESC) divided by the total amount of expected electricity demand (TD, CD), integrated over the entire year (8760 h) – calculated for both serving critical and total load profiles. Though the high priority and low priority load profiles are separated, this approach does not enforce a reliability threshold at sub-yearly scales (e.g. monthly, weekly, daily, or hourly) or at the individual household level.

$$TR_{k,l} = \sum_{i=1}^{8760} \sum_{j=1}^{h} \frac{EST_{i,j}}{TD_{i,j}} \tag{4}$$

$$CR_{k,l} = \sum_{i=1}^{8760} \sum_{j=1}^{h} \frac{ESC_{i,j}}{CD_{i,j}} \tag{5}$$

In order to find viable solutions, the model requires an input of desired reliability thresholds for both critical and total (critical plus non-critical) load profiles. This is the key capability represented in power management devices described to enable micro-grids with demand-side management: that electricity demand can first be disaggregated and prioritized – followed by the decision whether to serve or curtail this demand (at each hour in simulation). As defined by the consumer, critical loads are high priority loads that would be served first in any resource-constrained scenario; remaining, non-critical loads can be considered to have lower priority.

Given that it is unlikely that there exists one particular solution that would meet an exact reliability threshold, the model accepts reliabilities that are at least the input values. Using a two-dimensional search methodology, the algorithm then identifies the combination of the solar panel and battery where the system falls within the range of accepted reliability thresholds for both serving the critical and total load profiles; the outputs of the reliability values across available solar and battery capacities in the 'residential load' scenario are shown in Figs. 8 and 9. The z-axis represents the average yearly reliability in both graphs, with the x-y coordinate plane representing discrete values of available solar panels (in watts) and batteries (in amp-hours). In Fig. 8, the trends towards increasing reliability seems to be continuous in comparison to Fig. 9; the presence of discontinuities in the latter is because in this example use-case, the critical load profile is not serving any daytime loads, and is solely based on serving evening loads (in lights). Thus, for serving the modeled critical loads, the reliabilities are essentially near zero for smaller batteries.

The set of feasible solutions can be interpreted first by the values of each matrix that are greater than or equal to the reliability thresholds, and second by the overlap of those indices across both matrices. The optimal solution is found by using a two-dimensional search methodology to come up with these overlapping indices. The model's algorithm compares where the sets of identified indices intersect, meaning which combination of solar panel and battery capacity meets both total and critical reliability thresholds. To find the optimal solution, the last step is for the algorithm to pick the combination which has the least cost combination of the solar and battery assets ($c_{k,l}$) — taking into account the economies of scale for both solar modules ($/W) and batteries ($/kWh). The optimization heuristic employed is described in the following equations; note that $c_l = \$/\text{W}$, and $c_k = \$/\text{kWh}$ for respective solar and battery per unit costs, with the indices k and l corresponding to combinations of available solar module size (PV) and battery capacity (B), with a nominal battery voltage of $V = 12$ (with the default values for TR and CR at least 90% and 99%, respectively):

$$\begin{aligned} \min_{c} \quad & c_{k,l} = \frac{B \times c_k \times V}{1000} + PV \times c_l \\ & s.t. \quad TR_{k,l} \geq 90\% \\ & CR_{k,l} \geq 99\% \\ & k \in \{1 \ldots n\} \\ & l \in \{1 \ldots m\} \end{aligned}$$

For the final selected generation asset combination, in a 250 W solar panel and 100 Ah battery, the calculated reliabilities are 99.45% and 94.26% serving the critical and total load profiles, respectively; in this use-case of the model, the reliability thresholds

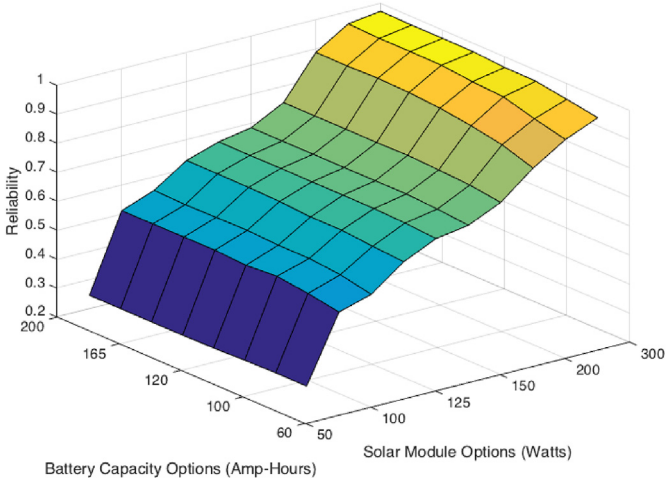

Fig. 8. Total Reliability vs. PV and Battery Capacities.

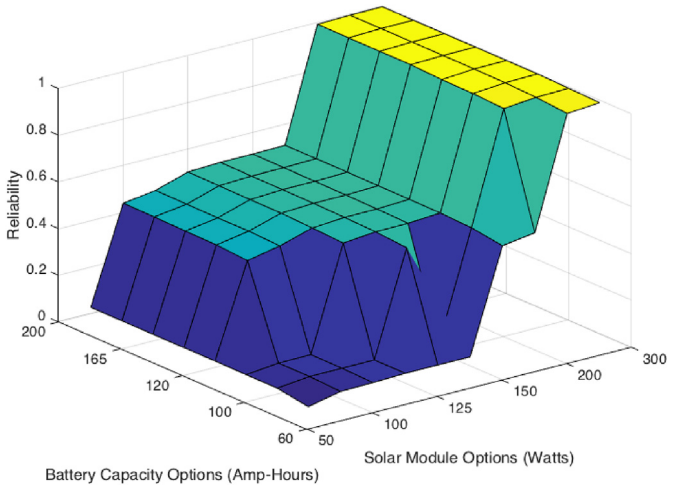

Fig. 9. Critical Reliability vs. PV and Battery Capacities.

are set to be 99% for the critical load profile, and 90% for the total profile. Reliability is essentially defined to be the average reliability served over the entirety of the year. Figs. 10 and 11 illustrate the calculated hourly reliability and compare the amount of non-served energy at each hour to the demand profiles (again, for both total and critical load profiles).

The top scatter plots in both figures show the hourly values for reliability, and the bottom plots show the comparisons between the non-served energy and expected demand profiles. For the critical reliability, the requisite threshold is higher, shown by the fact that nearly all of the hourly reliability values are near 1 (e.g. 100%) for serving the evening lighting loads. For the total reliability, the main hours of the year where reliability is lower is during the simulated peak periods of higher amounts of fan usage (again, induced in the demand profile construction by ambient temperatures and unable to be served by the available solar power). Though there are on the order of hundreds of hours where the total reliability is below 90%, in aggregate, the amount of energy served versus the amount of energy demanded meets the 90% reliability threshold when considering the entirety of the year.

Furthermore, though there may be many hours of the year when reliability is low, the magnitude of those values (in terms of watts) may be small — and thus not have a significant effect. Given that behavioral and real-time peak shifting effects are not taken into account in simulation, one way to view this metric is as a lower bound for the reliability provision; again, algorithms for real-time implementation of varied demand-side strategies in micro-grids is outside of the scope of the work presented here.

8. Economic and financial analysis of greenfield micro-grid

The feasible set is determined by the set of i and j indices that meet both critical and total load profile reliability thresholds, and the final step of the algorithm chooses the least cost combination of the solar panel and battery asset; note that each of values in each of the cells is calculated based on the objective function that relies on an exponential relationship of the per unit costs of batteries and solar panels. With five residential household demand profiles (including network losses associated with hardware), the availability of solar and battery combinations, and the set reliability thresholds of 99% for critical loads and 90% for total loads, the least cost selection of solar and battery assets comes out to be a **250W** panel and **100 Ah** battery — a combined cost of **$196.49** + **$134.47** = **$330.96**. The selection of high levels of reliability for micro-grids with real-time demand-side management show that reliability is not being sacrificed in order to be cost-competitive with conventional micro-grid approaches, as further discussed in the subsequent sections.

8.1. Additional micro-grid capital costs

The state-space matrices represent the available solar and

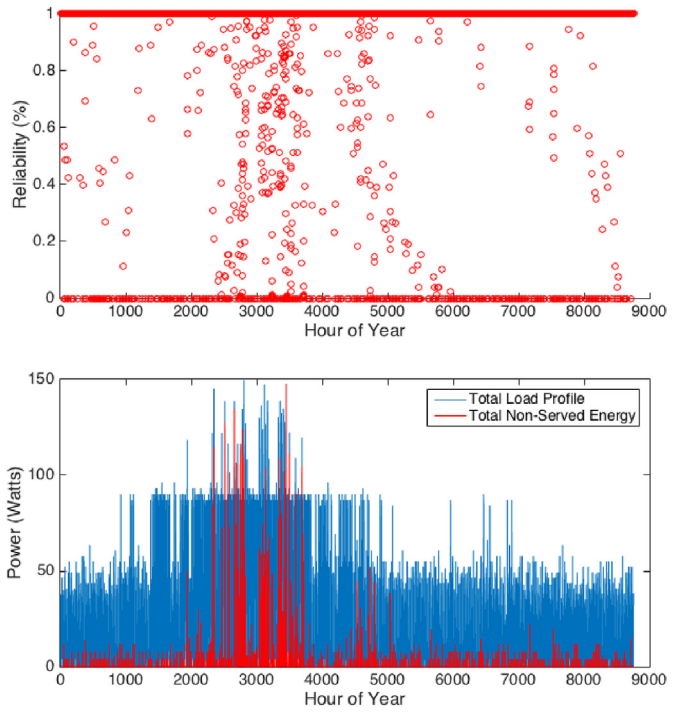

Fig. 10. Simulated hourly reliability: Total load profile (94.26%).

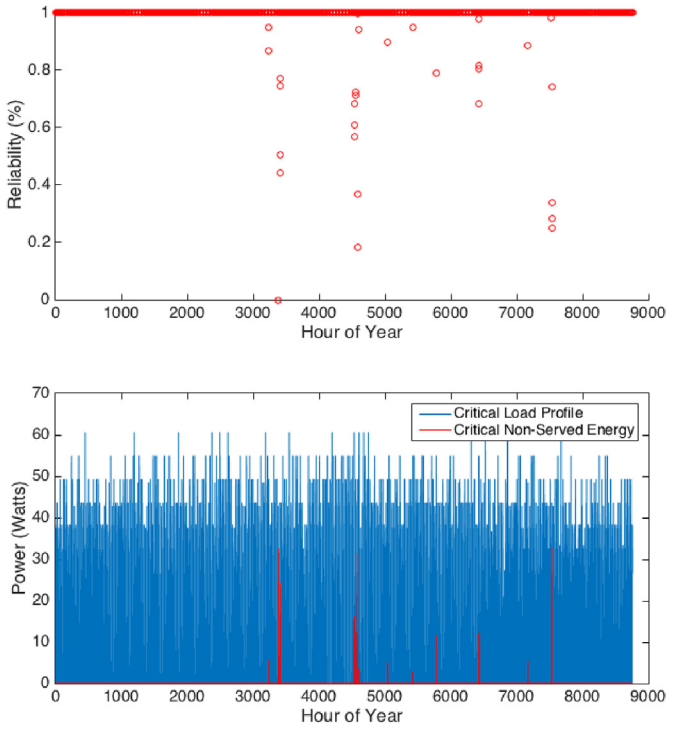

Fig. 11. Simulated hourly reliability: Critical load profile (99.45%).

battery combinations and are populated with average yearly reliabilities serving critical and total load profiles. The combination of the solar and battery, plus the costs included in Table 3 consist of the capital costs for the system.

Fig. 12 shows the distribution of capital costs in the nano-grid described. Total initial capital costs, comes out to be $542.06 – coming to a $2.17/W installed and a $108.41 per household for a five household installation (see Fig. 13).

8.2. Replacement costs based on equipment lifetime

In addition to the initial capital investment, the economic model takes into account replacement costs of the key assets in the network based on the lifetime of each asset (as shown in Table 4. In this case, the battery replacements are taken into account by taking the expected number of cycles in a particular year (based on the implementation of the rainflow counting algorithm previously described), and dividing that by the cycle lifetime; this gives the expected number of years that the battery will last given how it is cycled in the particular year simulated.

8.3. Financial model overview & results

The key financial inputs as shown in Table 5 are used in net present value (NPV) and levelized cost of electricity (LCOE) calculations. Over the lifetime of the system, the LCOE calculates all the recurring annual costs (such as maintenance, replacement, and initial capital costs) and is divided by the total amount of energy (in kWh) that the network served; note that a key assumption here is that the denominator value is assumed to be static, not taking into account demand growth and incrementally adding generation assets to meet increasing demand.

The model takes into account the capital costs, replacement costs, and maintenance costs for a micro-grid. Furthermore, there is assumed to be no capital (or operational) subsidy taken into account. In this use-case of the model, for the residential load profile scenario with respective total and critical load profile reliability thresholds at 90% and 99% serving five households, the *LCOE* is calculated to be $0.32/kWh (see Equation (15)). The numerator is based on the *NPV* of the cash outflows or costs (*C*), and the denominator is the sum of the entirety of the energy served (*EST*) in the micro-grid in each year, *y* (and not energy generated, which is typical for stand-alone photovoltaic systems). Note that the yearly discount rate used is 12% which is a considered to be reasonable

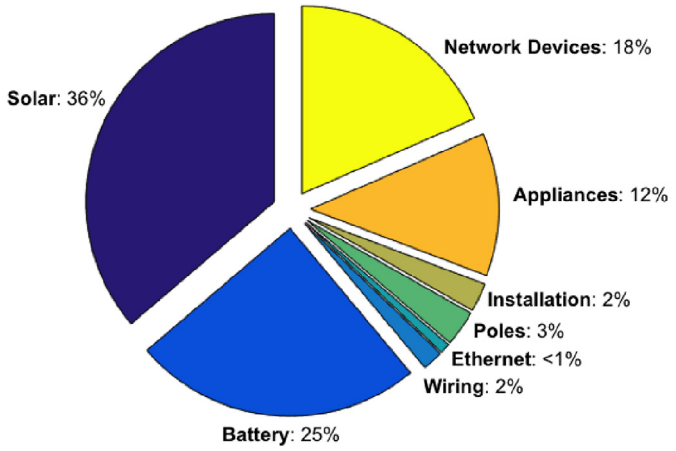

Fig. 12. Distribution of capital costs of micro-grid with optimized generation asset sizes.

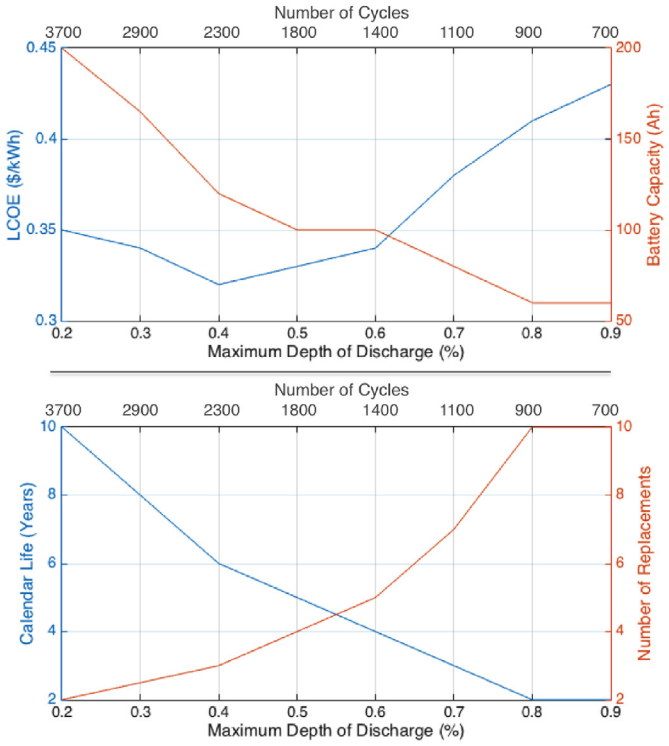

Fig. 13. Tradeoff between MDOD and cycle life with battery selection and replacement costs.

value for renewable energy projects in India as evaluated in Ref. [35]; further sensitivity analyses pertaining to varying financial parameters, such as monthly payments, discount rate, and payback period, can be found in Ref. [28].

$$NPV = \sum_{y=1}^{Y} \frac{C_y}{(1+d)^y} \tag{6}$$

$$LCOE = \frac{NPV}{\sum_{y=1}^{Y} \sum_{i=1}^{8760} EST_{i,y}} \tag{7}$$

Table 4
Lifetime of equipment assets.

Asset	Lifetime
Solar Module	15 years
Battery [60% MDOD]	1400 cycles [Fig. 7]
Poles	5 years
Appliances	2 years
Network Devices	5 years

Table 5
Key financial inputs.

Parameter	Value
Yearly Discount Rate (d)	12% [35]
Monthly Discount Rate (d′)	0.95%
Payback Period (P)	5 years
System Lifetime (Y)	20 years
Maintenance Rate	2.5%/year of C_0
Exchange Rate	Rs. 66/ $

9. Sensitivity analysis to key model inputs

The previous sections have described the series of computational steps and initial results for a particular use-case in assessing the design selection of generation assets in micro-grids with demand-side management capabilities; as a reference, these steps are depicted in the process flow diagram in Fig. 1. This model is based on a variety of inputs – the selection of which have underlying inter-dependencies that impact results of the model. To summarize, the use-case of the model presented assumes following key inputs:

- **Demand Inputs:** Five customers/households' aggregated residential load profiles taken for a representative year (see Table 1);
- **Solar Resource:** Historical solar irradiance in Jharkhand, India [31];
- **Solar/Battery Choices:** Available solar panels and lead-acid batteries per distributor availability, and associated costs;
- **Battery Operation:** Default value for maximum depth of discharge (MDOD) for lead-acid battery of 60%, corresponding to 1400 cycles (see Fig. 7);
- **Reliability Thresholds:** Baseline average yearly reliability thresholds for serving total (90%) and critical (99%) load profiles (see Figs. 8 and 9);
- **Cost Inputs:** Values for appliances, power management devices, network, etc. based on prices gathered from local shops in Jamshedpur, India (see Table 3);
- **Equipment Lifetime:** Lifetime of equipment assets, in years, that dictates replacement costs (see Table 4);
- **Financial Inputs:** Discount rate, payback period, and system lifetime which impact business model viability (see Table 5).

The purpose of this section is to illustrate some of the complex underlying relationships between variables to get a better sense of what of these aforementioned inputs – and why – impact both the technical and economic outputs.

9.1. Effect of maximum depth of discharge and cycle life on levelized cost of electricity

Not only is the selection and operation of a battery important, so is the allowable depth of discharge and its relationship to cycle life. Therefore, the key tradeoff to consider is that deeper depths of discharge can allow for a smaller battery size, but requires replacing the battery more frequently in turn. The two plots in Fig. 14 aim to capture this relationship based on the model constructed. The top plot shows that for an increasing depth of discharge (corresponding to a decrease cycle life), the choice of battery capacity decreases. However, the levelized cost of electricity forms a discontinuous parabolic-like shape (given that only discrete values for battery capacities are made available in the construction of the model), capturing the fact that increasing the depth of discharge requires more frequent replacements and negatively affects costs. This is a good indicator on the fact that many lead-acid battery installations aim to take into account some notion of the depth of discharge and cycle life effects. The bottom plot shows precisely the increasing number of replacements over a 20 year system lifetime based on the decreasing calendar life of a battery. Note that the assumptions on the choice of MDOD and cycle counting are implemented in the form of the MDOD-constraint and the rainflow counting algorithm with battery's lifetime in years rounded based on the expected cycle life and the number of cycles expected for one year.

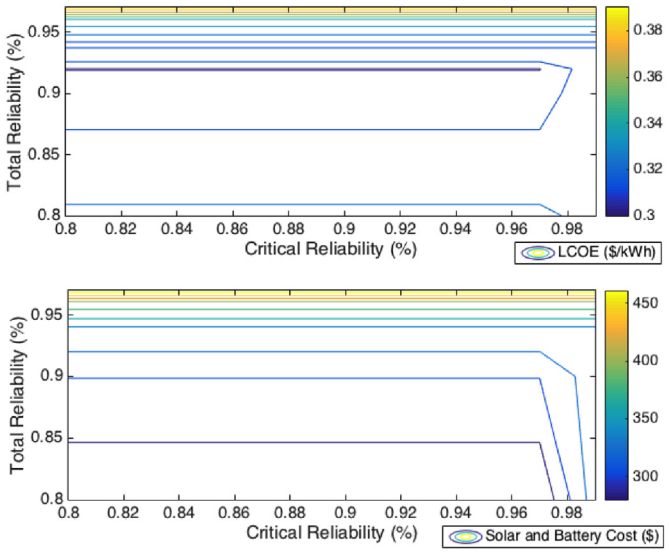

Fig. 14. Effects of reliability thresholds on cost metrics.

9.2. Effect of reliability thresholds on costs and generation asset selection

Thus far, the use-case presented herein has shown that for meeting total and critical reliability thresholds of 90% and 99% for five households' residential load profiles, a least-cost combination of a 250 W panel and 100 Ah battery can meet those requirements.

Fig. 16 shows two contour plots assessing the relevant cost parameters as a function of varying the total and critical reliability thresholds from 80% to 99%. For the most part, the top plot shows that the LCOE and capital costs (both per unit and combined total of generation assets) do increase with increasing reliabilities. The first interesting point is that the critical reliability only starts to affect the costs towards the end of the reliability spectrum; recall that the definition of critical loads are evening lights, showing that there is a minimum battery requirement for even unacceptably low levels of reliability. Second, this top plot shows that the costs are not entirely monotonically increasing as the reliability thresholds increase. Again, the model is optimizing for the least cost combination of both the solar panel and the battery subject to meeting reliability thresholds – and there may be multiple combinations that are feasible solutions. Thus, the 'lumpiness' of having only discrete combinations (and thus costs) of available solar panels and batteries as reliability thresholds are incrementally increased is the most plausible explanation for this. Fig. 15 aims to illustrate this argument, showing that for the 80 available pairs of solar panels and lead-acid batteries based on the initialized state-space, the varying proportion of the solar costs in relation to the combined solar module and battery capacity costs.

Fig. 16 explicitly shows the selection of the solar panel (top plot) and battery capacity (bottom plot) that correspond to total and critical reliability thresholds. These plots support the previous arguments in that though there may be multiple solutions, in some instances the model selects a larger solar panel and a smaller battery as total reliability (which includes the key daytime load of the fan) increases. However, to get to the high levels of critical reliability, both the battery and solar panel capacities have to be increased.

Note that the common $/W metric used in evaluating costs of power systems is intentionally omitted in this context, as it takes into account the rated power of the solar panel but not the battery

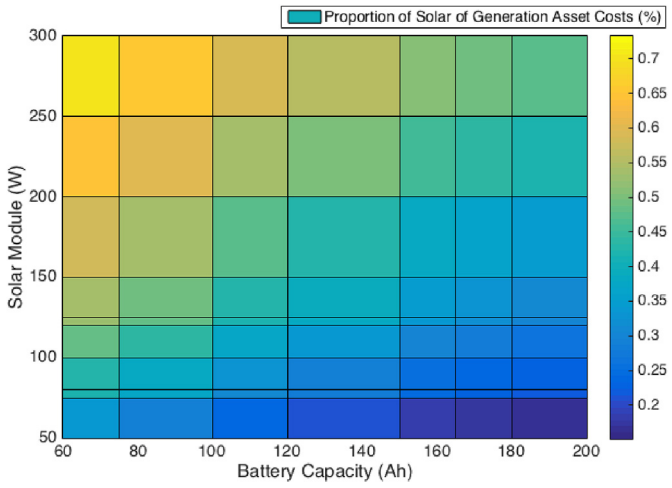

Fig. 15. Proportion of solar costs across available solar/battery state-space.

in the denominator. Thus, for various combinations that may meet the same reliability thresholds, there are combinations present that may increase the solar panel while decreasing (or keeping the same) battery capacity – which may have a net effect of decreasing the $/W. Though this per unit metric is commonly used when assessing standalone, grid-connected, photovoltaic systems, it may not be an appropriate metric in micro-grids where the storage requirements represent a significant amount of the costs in the numerator.

10. Generation asset sizing results & comparison

As discussed as part of the motivation for this work, one of the main drawbacks of conventional electricity access approaches is the tendency – due to a lack of demand-side management and network control capabilities – to over-size generation assets. In discussions with solar home system equipment manufacturers and micro-grid operators, the reasons for over-sizing systems (which drives costs) include to maintain brand reputation and to ensure autonomous operation of a micro-grid during periods of low solar irradiance throughout worst case scenarios. Many such companies operating in off-grid, rural areas rely on integrating available equipment/components in nearby urban or peri-urban areas. However, access to the specific methods, data on in-field performance, and assumptions (e.g. local solar resource, daily load, variability, etc.) equipment manufacturers used for generation asset sizing are not available – thus making proper comparisons to benchmark the accuracy and costs of this model difficult.

Typical micro-grids in India are on the order of 30 households and provide 4–5 h of evening electricity service with basic loads such as LED's and mobile phone – constituting as the 'peak' load per household [16]. To benchmark the results from the model, the output of the least-cost generation asset sizes for serving such a micro-grid's load profile, with 99% reliability, is a 200 W solar panel and a 150 Ah lead-acid battery. Again, this is the result from the least-cost combination of generation assets that meet the reliability threshold – but note that for this use-case, 14 combinations of solar panels and battery capacities meet a 99% reliability threshold; these various combinations are shown (with combined costs) in Table 6. These results are on the order of generation asset sizes typically seen in such micro-grids, e.g. batteries in a 150 Ah-200 Ah range and solar panels in a 200 W–300 W range [16].

With the addition of a 12 W fan per household and extending the state-space beyond the largest solar panel (300 W) and battery (200 Ah) to be multiples of 200 W panels and 100 Ah batteries, the model outputs **1,200W** worth of solar panels (6×200 W) and **500 Ah** of lead-acid battery capacity (5×100 Ah) – to achieve reliability to be above 99%. The combined costs of these generation assets is **$1621**. However, if we separate the cell phone charger and the fan to be non-critical loads, and allow for a 90% reliability threshold to meet the total load profile (keeping the 99% critical reliability threshold constant), the selection of the generation assets is **1,000W** of solar panels (5×200 W) and **300 Ah** of battery capacity (3×100 Ah) – a reduction of one 1×200 W solar panel and 2×100 Ah lead-acid batteries. In terms of capital costs, this combination of generation assets costs **$1,194**, a difference of **$427** (or a reduction of 26% in generation asset costs). Conducting such simulations with a conventional micro-grid not only helps validate the outputs of the model, but further illustrates the potential for demand-side management to more optimally size generation assets, thus reducing the costs for micro-grids.

Again, both the optimally sized system with demand-side management and the over-sized system yield $\geq$ 99% reliability for

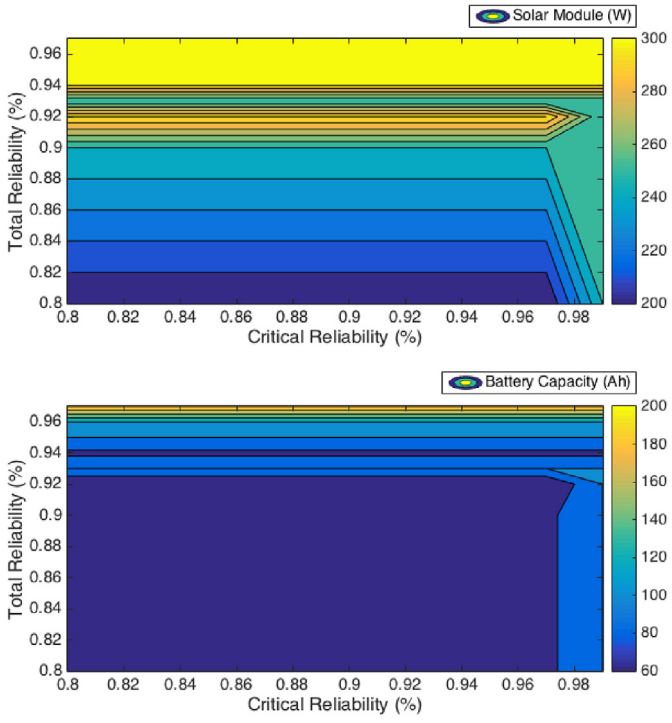

Fig. 16. Solar module and battery capacity choice based on reliability.

Table 6
Available solar/battery combinations meet $\geq$ 99% reliability for typical micro-grid.

Battery Size (Ah)	Solar Panel (W)	Combined Cost ($)
150	200	348.77
165	200	364.34
100	300	368.85
180	200	379.33
150	250	387.12
120	300	392.11
200	200	398.46
165	250	402.69
180	250	402.69
150	300	425.01
200	250	436.81
165	300	440.58
180	300	455.57
200	300	474.70

the high-priority critical loads (e.g. evening lighting). But by incorporating demand-side management, a lower reliability threshold of 90% serving the total loads (including fans and cell phone chargers) allows for a reduction in capital costs for the micro-grid.

11. Conclusion & future work

As discussed, there have been numerous previous efforts focused on techno-economic analyses of micro-grids of various configurations. This differentiated approach shared herein provides a realistic and contextually relevant understanding of the performance and costs of solar and battery-based micro-grids with demand-side management capabilities. This paper walks through a series of sequential, computational steps, encompassing battery model simulations to model such micro-grids – with the overarching objective to find the least cost solar and battery combination that meets reliability thresholds for an aggregated demand profile.

In any model, the results are a direct function of the quality of the inputs. The model construction framework and the simulation results shared herein have aimed to be contextually relevant, incorporating available generation assets and cost inputs as seen in Jamshedpur, in the Indian state of Jharkhand. Furthermore, the aim of the model is that it can be used in other contexts with changes of the inputs, such as the number of users, expected wiring distance or gauge, etc. – but is built solely on the basis of integrating solar and lead-acid batteries within a low-voltage, DC network. After yearly simulations of each combination of solar and battery capacities with dispatch decisions made at each hourly timestep, the key decision of the model – in the selection of optimized solar and battery assets – is based on the least cost combination that meet minimum thresholds of reliability. In this work, reliability has been considered as the ratio between the cumulative electricity served (incorporating line and efficiency losses in the network) versus the expected electricity demand – a reasonable approximation for the purposes of simulation.

Future modeling work in this realm should focus explicitly taking into account the potential for reducing operational costs when compared to conventional micro-grids. This could further supplement the cost-benefit argument for micro-grids with demand-side management; operational costs could be reduced by restricting types of loads being connected, monitoring electricity theft, maintaining network stability across households and heterogeneous appliances, incorporating forecasts into real-time dispatch decisions to effectively manage battery state-of-charge, and requiring mobile payments for continued service instead of relying on door-to-door collections.

In practice, understanding and quantifying the value of reliability is a significant and important challenge. Micro-grid equipment or service provider's rationale for over-sizing systems is to minimize the probability of the event that a load (and thus, a household activity) is not served in its entirety. Similar to demand response efforts in the developed world, the goal of this effort is to separate an acceptable level of service for critical loads from the remaining loads. Yet understanding these thresholds for what is acceptable from consumers' perspectives need to be thoroughly understood in advance of any implementation.

Thus, it is critical to recognize the on-the-ground reality and associated challenges of implementing micro-grids with demand-side management in rural areas such as in Jharkhand, India. Specifically, implementation will require a more nuanced understanding of households' load preferences and priority, along with the implications that the curtailment of specific loads has on users' perception of quality of service and willingness-to-pay [28]. Additional work should investigate whether such nano-grids can alleviate high customer acquisition costs that are common with centralized micro-grids, how individuals can also be incentivized to invest in their own electricity infrastructure by monetizing transactions amongst neighbors, and over time, whether such micro-grids can be connected together to effectively utilize excess solar generation and manage demand.

In conclusion, the methodology presented considers the technical design, operation, economic value, and cost competitiveness of low-cost solar micro-grids with demand-side management. This analysis includes the incremental costs of the required power management devices to enable such micro-grids, and evaluates the capital and operational costs for a five-household installation based on distributor availability of solar panels and lead-acid batteries in Jharkhand, India. The key result shared is that in comparison to conventional micro-grids for electricity access, demand-side management capabilities can reduce the number of requisite solar panels and batteries due to the integration of real-time management and control – an encouraging result for the next generation of electricity access technologies and implementation approaches.

Acknowledgements

The authors would like to thank the Tata Center for Technology and Design at MIT for financial support and the Tata Steel Rural Development Society in Jamshedpur, India for being integral partners in this work.

References

[1] Alstone P, et al. Decentralized energy systems for clean electricity access. Nature Climate Change: Perspective. Mar. 2015.
[2] Schnitzer D, et al. Microgrids for Rural Electrification: a critical review of best practices based on seven case studies. United Nations Foundation; Feb. 2014.
[3] Achieving universal electrification in India. Institute for Transformative Technologies (ITT); Apr. 2016.
[4] Harper M. Review of strategies and technologies for demand-side management on isolated mini-grids. Schatz Energy Research Center, Humboldt State University; Mar. 2013.
[5] Network optimized distributed energy systems (NODES): funding opportunity announcement. Advanced Research Projects Agency - Energy (ARPA-E); Feb. 2015.
[6] Palma-Behnke R, et al. A microgrid energy management system based on the rolling horizon strategy. IEEE Trans Smart Grid June 2013;4(2):996–1006.
[7] Mazzola S, et al. Assessing the value of forecast-based dispatch in the operation of off-grid rural microgrids. Appl Energy Aug 2017;108:116–25.
[8] Ou TC, et al. Dynamic operation and control of microgrid hybrid power systems. Energy Oct. 2014;66(10), 314323.
[9] Strawser D, et al. A market for reliability for electricity scheduling in developing world microgrids. In: Proceedings of the 2015 international conference on autonomous agents and multiagent systems; May 2015. p. 1833–4.
[10] Inam W. Architecture and system analysis of microgrids with peer-to-peer electricity sharing to create a marketplace which enables energy access. In: 9th international conference on power electronics; June 2015.
[11] Akinyele DO, Rayudu RK. Techno-economic and life cycle environmental performance analyses of a solar photovoltaic microgrid system for developing countries. Energy Aug. 2016;109:160–79.
[12] Thomas D, et al. Optimal design and techno-economic analysis of an autonomous small isolated microgrid aiming at high RES penetration. Energy Dec. 2016;116:364–79.
[13] Bhatt A, et al. Feasibility and sensitivity analysis of an off-grid micro hydro-photovoltaic-biomass and bio- gas-diesel-battery hybrid energy system for a remote area in Uttarakhand state, India. Renew Sustain Energy Rev Aug. 2016;61:53–69.
[14] Alireza HM, et al. Techno-economic feasibility of photovoltaic, wind, diesel and hybrid electrification systems for off- grid rural electrification in Colombia. Renew Energy Nov. 2016;97:293–305.
[15] Dong W, et al. Optimal sizing of a stand-alone hybrid power system based on battery/hydrogen with an improved Ant colony optimization. Energies Oct. 2016;9(10).
[16] Campanella A. An analysis of the viability and competitiveness of DC microgrids in Northern India. Master's of Science Thesis. Engineering Systems Division: Massachusetts Institute of Technology; Aug. 2013.
[17] Han X, et al. Economic evaluation of grid-connected micro- grid system with photovoltaic and energy storage under different investment and financing

models. Appl Energy Dec. 2016;184:103–18.
[18] Manwell JF, McGowan JG. Lead acid battery storage model for hybrid energy systems. Sol Energy 1993;50(5):399–405.
[19] N. DiOrio et al. Technoeconomic modeling of battery energy storage in SAM. National Renewable Energy Laboratory.
[20] Lee M. Cost versus reliability sizing strategy for isolated photovoltaic microgrids in the developing world. Renew Energy Sept. 2014;69:16–24.
[21] Louie H, Dauenhauer P. Effects of load estimation error on small-scale off-grid photovoltaic system design, cost and reliability. Energy Sustain Dev Oct. 2016;34:30–43.
[22] Electric Power Research Institute (EPRI). Residential off-grid and storage systems: a case study comparison of on-grid and off-grid power for residential consumers. Jan. 2016. http://www.epri.com/abstracts/Pages/ProductAbstract.aspx?ProductId=000000003002009150.
[23] Boait P, et al. Estimation of demand diversity and daily demand profile for off-grid electrification in developing countries. Energy Sustain Dev Dec. 2015;29:135–41.
[24] Mehra Varun. GitHub repositories. 2017. https://github.com/vmehra813?tab=repositories.
[25] Zhou P, et al. Reliability and economic evaluation of power system with renewables: a review. Renew Sustain Energy Rev 2016;58:537–47.
[26] Sullivan MJ, et al. Updated value of service reliability estimates for electric utility customers in the United States. Jan. 2015. https://mpbl.gov/sites/all/files/value-of-service-reliability-final.pdf.pdf.
[27] Acuna LG, et al. Measuring reliability of hybrid photovoltaic-wind energy systems: a new indicator. Renew Energy June 2017;106:68–77.
[28] Mehra V. Optimal sizing of solar and battery assets in decentralized microgrids with demand-side management. Master's Thesis. Department of Electrical Engineering, Computer Science, Institute for Data Systems, and Society: Massachusetts Institute of Technology; Feb. 2017.
[29] Universal Energy Access Research Group. The Reference Electrification Model. http://universalaccess.mit.edu.
[30] Ellman D. The reference electrification model: a computer model for planning rural electricity access. Master's project. Engineering Systems Division: Massachusetts Institute of Technology; May 2015.
[31] National Renewable Energy Laboratory (NREL). PV Watts Calculator. http://pvwatts.nrel.gov/.
[32] Inam W. Adaptable power conversion for grid and micro- grid applications. PhD Dissertation. Department of Electrical Engineering and Computer Science: Massachusetts Institute of Technology; May 2016.
[33] Cavanagh K, et al. Transient stability guarantees for ad hoc dc microgrids. Oct. 2017.
[34] Downing SD, Socie DF. Simple rainflow counting algorithms. Int J Fatig 1982;4:3140.
[35] Meier P, et al. The design and sustainability of renewable energy incentives: an economic analysis. Directions in development. World Bank; 2015.